International Journal of Current Engineering and Technology
E-ISSN 2277 – 4106, P-ISSN 2347 – 5161

Available at http://inpressco.com/category/ijcet

Research Article

Modeling and Simulation of Solar PV System for Water Pumping

Abobaker Mahdi Abobakr Nasar* and Jyoti Shrivastava

Electrical Engineering Department, SHUATS, Allahabad, India

Received 14 Aug 2018, Accepted 16 Oct 2018, Available online 18 Oct, **Vol.8, No.5 (Sept/Oct 2018)**

Abstract

Solar Photovoltaic (PV) systems are having growing importance in present time of our power system due to its non-polluting, minimum maintenance, and free fuel characteristics. Photovoltaic systems are comprised of photovoltaic cells, devices that convert light energy directly into electricity. Since the source of light is usually the sun, they are often called solar cells. Photovoltaic modules are widely used in induction motor applications. One of these applications may be in water pumping system. The boost converter has been used boosting the weak output voltage generated by the cells. Boosting of voltage is being done in reality by the maximum power point technique (MPPT). In this technique the automated tracking to give the highest output power is done by an algorithm. This generated power is fed to a boosting load across which the boosted output voltage is being received. This output voltage is then fed to operate a induction motor, driving a pumping system.

Keywords: *Photovoltaic system, converter DC-DC, induction motor, 3 phase inverter and MPPT technology*

1. Introduction

Solar energy is the most low cost, competition free, universal source of energy as sun shines throughout. This energy can be converted into useful electrical energy using photovoltaic technology. The steady state reduction of price per peak watt and simplicity with which the installed power can be increased by adding panels are attractive features of PV technology. Among the many applications of PV energy, electric vehicle is the most promising. In a PV pump storage system, solar energy is stored, when sunlight is available as potential energy in water reservoir and consumed according to demand. There are advantages in avoiding the use of large banks of lead acid batteries, which are heavy and expensive and have one fifth of the lifetime of a PV panel. A number of experimental induction motor driven PV electric drive are already in use in several parts of the world, but they suffer from maintenance problems due to the presence of the commutator and brushes.

Hence a pumping system based on an induction motor can be an attractive proposal where reliability and maintenance-free operations with less cost are important. The effective operation of Induction motor is based on the choice of suitable converter-inverter system that is fed to Induction Motor. Converters like Buck, Boost and Buck-Boost converters are popularly used for photovoltaic systems. But these converters are limited to low power applications. For PV applications like pumping these converters could do a good job as pumping is carried out at high power. Thus a new push pull converter which is two switch topology can do justice by giving a high power throughout. The Induction Motors are the AC motors and hence from converter, an inverter system is also required to obtain an AC voltage. This inverter is chosen based on its advantages and it is fed to induction motor. Photovoltaic technology is one of the most promising for distributed low-power electrical generation. The steady reduction of price per peak watt over recent years and the simplicity with which the installed power can be increased by adding panels are some of its attractive features.

2. System Description and Modelling

A) Solar Cell Model

a) Equivalent circuit of a solar cell

n order to analyze the electronic behavior of a solar cell, an electrical equivalent model is considered. An ideal PV cell may be considered as a current source in parallel with a diode. In practice a PV cell is not ideal, so a shunt resistance and a series resistance component are added to the model. The resulting equivalent circuit is shown in the Figure 1.

*Corresponding author **Abobaker Mahdi Abobakr Nasar** is a Research Scholar (ORCID ID: 0000-0002-8731-9043); **Jyoti Shrivastava** is working as Assistant Professor
DOI: https://doi.org/10.14741/ijcet/v.8.5.16

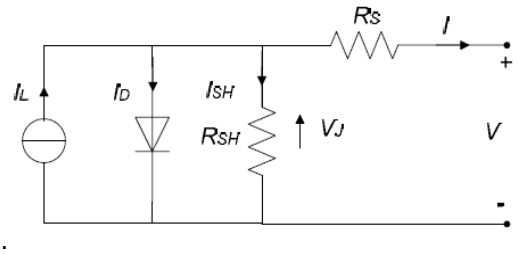

Fig 1 Equivalent circuit

b) Characteristic equations

In this equivalent circuit, the PV cell is considered as a current source with the photovoltaic effect. The output current is expressed as:

$$I(t) = I_L(t) - I_D(t) - I_{SH}(t) \quad (1)$$

Where

I: output current (amperes),
I_L: photo generated current (amperes), ID: diode current (amperes),
I_{SH}: shunt current (amperes).

The current through these elements is governed by the voltage across them:

$$V_j(t) = V(t) + I(t)R_s \quad (2)$$

Where,

V_j : voltage across the diode and the resistor RSH (volts),
V : voltage across the output terminals (volts),
I : output current (amperes),
R_S : series resistor (Ω).

With the Shockley diode equation, the current through the diode is expressed as:

$$I_D(t) = I_0\left\{\exp\left[\frac{qV_j(t)}{nkT}\right] - 1\right\} \quad (3)$$

Where

I_0 : reverse saturation current (amperes),
n : diode ideality factor (1 for an ideal diode),
q : elementary charge (1.6022*10-19 coulomb),
k: Boltzmann's constant (1.3806*10-23 J/K), T : absolute temperature and 0.0259 Volt at 25°C.
With the Ohm's law, the current through the shunt resistor is expressed as:

$$I_{SH}(t) = \frac{V_j(t)}{R_{SH}}$$

Where R_{SH} : shunt resistor (Ω).

$$I(t) = I_L(t) - I_0\left\{\exp\left[\frac{q(V(t) + I(t)R_s)}{nkT}\right] - 1\right\} - \frac{V(t) + I(t)R_s}{R_{SH}} \quad (4)$$

For a given voltage ($V(t)$ the equation may be solved to determine the output current I (t) . Because the equation involves the current on both sides in a transcendental function the equation has no general analytical solution. However it is easily solved by using numerical methods. Since the parameters I_0, n, R_S, and R_{SH} cannot be measured directly, a characteristic equation is generally used with a nonlinear regression to extract the values of these parameters on the basis of their combined effect on the PV cell behavior.

c) Photovoltaic cell model

When the cell is operated in short circuit, V = 0 and the current I (t) through the terminals is defined as the short-circuit current $(I(t))_{SC}$. For a high-quality PV cell (low value of RS and $I0$, and high value of RSH) the short-circuit current ISC is expressed as:

$$I_{SC}(t) \approx I_L(t)$$

By taking into account the effect of the irradiance and the temperature, the current I_{SC} is expressed as

$$I_{SC}(t) = I_{SCS}\frac{G(t)}{G_s}[1 + \Delta I_{SC}(T(t) - T_s)] = I_L(t) \quad (5)$$

With G: irradiance (W / m^2),
T: cell temperature (K),
I_{scc} : short circuit current measured in Standard Test Conditions (STC),
Gt : Standard illumination: 1000 W / m^2,
Tt : standard temperature: 298.15 K.
ΔI_{sc} : temperature coefficient of short circuit current.

When the cell is operated in open circuit and I = 0, the voltage across the output terminals is defined as the open-circuit voltage (VOC). Assuming the shunt resistor (RSH) is high enough to neglect the final term of the characteristic equation (R.I-5), the open-circuit voltage is expressed as:

$$V_{OC}(t) \approx \frac{kT}{q}\ln\left(\frac{I_L(t)}{I_0} + 1\right) \quad (6)$$

In an open-circuit condition: VOC = V and I = 0, the equation (R.I-1) can be written as:

$$I_L(t) = I_D(t) + I_{SH}(t) = I_{sat}\left[\exp\left(\frac{V_{oc}(t)}{V_t}\right) - 1\right] + \frac{V_{oc}(t)}{R_{SH}} \quad (7)$$

With

$$V_t = \frac{AkT}{q}$$

and A the Ideal factor of the diode, The saturation current is defined as:

$$I_{sat} = \frac{I_L(t) - \frac{V_{oc}(t)}{R_{SH}}}{\exp(\frac{V_{oc}(t)}{V_t}) - 1} \quad (8)$$

The open-circuit voltage is expressed as:

$$V_{OC} = V_{OCS} + \Delta V_{OC}(T - T_s) \quad (9)$$

With V_{OCS}: open-circuit voltage in STC,
ΔV_{OC}: temperature coefficient of open circuit voltage.
Note: The resistors and the ideal factor are influenced by the temperature. In
order to simplify the model, these values are set in STC.

d) Maximum Power Point Tracking (MPPT)

A solar cell may operate over a wide range of voltages (V) and currents (I). By increasing the voltage of an irradiated cell continuously from zero (a short circuit) to a very high value (an open circuit) the maximum-power point can be determined. The point that maximizes the product V, I is achieved when the cell delivers the maximum electrical power for the received level of irradiation.

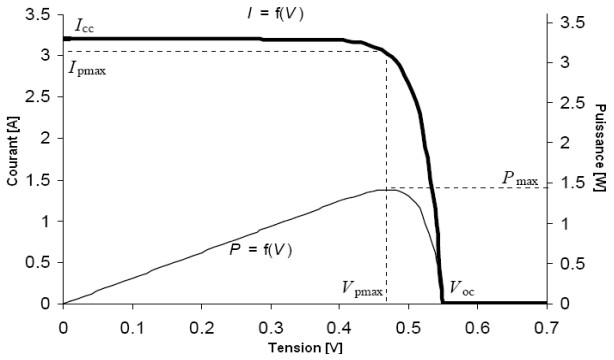

Fig.2 I= f(V) and P= f(V) characteristics of a PV Cell

The maximum power point varies with the incident illumination. For large PV systems, a maximum power point tracker tracks the instantaneous power by continually measuring the voltage and current. It uses this information to dynamically adjust the voltage so that the maximum power is always transferred, regardless of the variation in lighting. The MPPT control may be processed by using different algorithms. Perturbation and observation (P&O) and Incremental conductance are the most used algorithms.

e) Characteristics of PV model

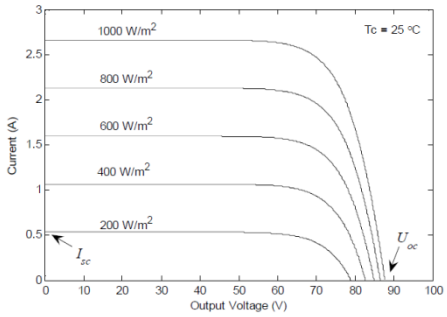

Fig .3: I-V characteristic curves of the PV mode under different irradiances

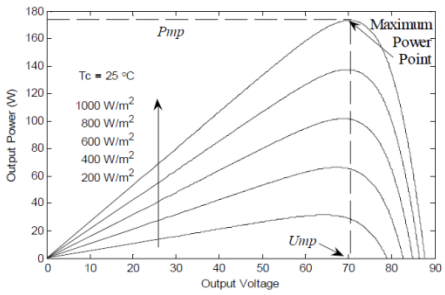

Fig.4 P-V characteristic curves of the PV model under different irradiances

f) Temperature Effect on the Model Performance

The effect of the temperature on the PV model performance is illustrated in Figures 4 and 5. From these two figures, it is noted that the lower the temperature, the higher is the maximum power and the larger the open circuit voltage. On the other hand, a lower temperature gives a slightly lower short circuit current.

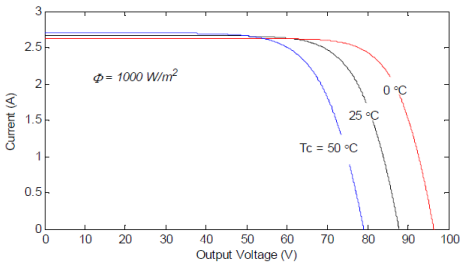

Fig.5 I-V characteristic curves of the PV model under different temperatures

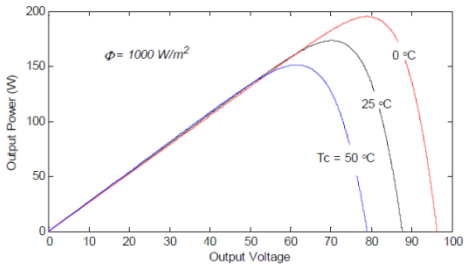

Fig.5 P-V characteristic curves of the PV model under different temperatures

B) Dynamic model of induction motor

The stator of induction motor consists of three phase balanced distributed windings with each phase separated from other two windings by 120 degrees in space. When current flows through these windings, three phase rotating magnetic field is produced. The dynamic behaviour of the induction machine is taken into account in an adjustable speed drive system using a power electronics converter. This machine constitutes an element within a feedback loop. Study of the dynamic performance of the machine is complex due to coupling effect of the stator and rotor windings; also the coupling coefficient varies with rotor position. So a set of differential equations with time varying coefficients describe the machine model. To derive the dynamic model of the machine, the following assumptions are made:

1) No magnetic saturation;
2) No saliency effects i.e. machine inductance is independent of rotor position;
3) Stator windings are so arranged as to produce sinusoidal mmf distributions;
4) Effects of the stator slots may be neglected;
5) No fringing of the magnetic circuit
6) Constant magnetic field intensity, radially directed across the air-gap;
7) Negligible eddy current and hysteresis effects;

A balanced three phase supply is given to the motor from the power converter. For dynamic Modeling of the motor two axes theory is used. According to this theory the time varying parameters can be expressed in mutually perpendicular direct (d) and quadrature (q) axis. For the representation of the d-q dynamic model of the machine a stationary or rotating reference frame is assumed.

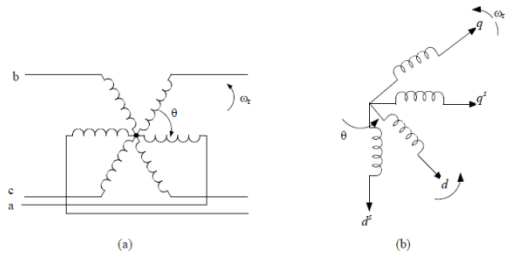

Fig.6 (a) Coupling effect in stator and rotor winding of motor (b) Equivalent two-phase machine

In stationary reference frame the d^s and q^s axes are fixed on the stator, whereas these are rotating at an angle with respect to the rotor in rotating reference frame. The rotating reference frame may either be fixed on the rotor or it may be rotating at synchronous speed. In synchronously rotating reference frame with sinusoidal supply the machine variables appear as dc quantities in steady state condition.

Axes transformation

(a) Three phase to two phase transformation

A symmetrical three phase machine is considered with stationary *as-bs-cs* axes at 120 Degree apart as shown in fig.3.2.

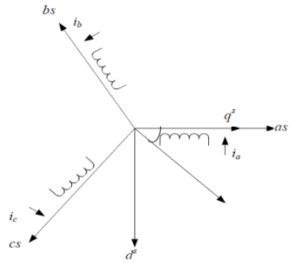

Fig.7 as- bs - cs to $d^s - q^s$ axis transformation (θ = 0)

The voltages v_{as}, v_{bs}, v_{cs} are the voltages of as, bs, cs phases respectively. Now assuming that the stationary d^s-q^s axes are oriented at θ angle as shown and the voltages along d^s -q^s axes to be vds^s, vqs^s respectively, the stationary two phase voltages can be transformed to three phase voltages according to the following equations:

$$v_{as} = v_{qs}^s \cos\theta + v_{ds}^s \sin\theta \quad (10)$$

$$v_{bs} = v_{qs}^s \cos(\theta - 120) + v_{ds}^s \sin(\theta - 120) \quad (11)$$

$$v_{cs} = v_{qs}^s \cos(\theta + 120) + v_{ds}^s \sin(\theta + 120) \quad (12)$$

The phase voltages in matrix form can be written as;

$$\begin{bmatrix} v_{as} \\ v_{bs} \\ v_{cs} \end{bmatrix} = \begin{bmatrix} \cos\theta & sin\,\theta & 1 \\ \cos(\theta - 120) & \sin(\theta - 120) & 1 \\ \cos(\theta + 120) & \sin(\theta + 120) & 1 \end{bmatrix} \begin{bmatrix} v_{qs}^s \\ v_{qs}^s \\ v_{os}^s \end{bmatrix}$$

By inverse transformation, v_{qs}^s and v_{qs}^s can be written in terms of three phase voltages in matrix form as follows:

$$\begin{bmatrix} v_{qs}^s \\ v_{qs}^s \\ v_{os}^s \end{bmatrix} = \frac{2}{3} \begin{bmatrix} \cos\theta & \cos(\theta - 120) & \cos(\theta + 120) \\ \sin\theta & \sin(\theta - 120) & \sin(\theta + 120) \\ 0.5 & 0.5 & 0.5 \end{bmatrix} \begin{bmatrix} v_{as} \\ v_{bs} \\ v_{cs} \end{bmatrix}$$

Where v_{os}^s = zero sequence component which may or may not present. For convenient q^s axis is aligned with the *as*-axis i.e. θ = 0 and zero sequence component is neglected. So the transformation relations are reduced to

$$v_{as} = v_{qs}^s \quad (13)$$

$$v_{bs} = -\frac{1}{2} v_{qs}^s - \frac{\sqrt{3}}{2} v_{ds}^s \quad (14)$$

$$v_{bs} = -\frac{1}{2} v_{qs}^s + \frac{\sqrt{3}}{2} v_{ds}^s \quad (15)$$

$$v_{qs}^{s} = v_{as} \quad (16)$$

$$v_{ds}^{s} = -\frac{\sqrt{3}}{2}(v_{bs} - v_{cs}) \quad (17)$$

C) 3.8 Voltage source inverter

In VSIs the input voltage is maintained constant and the amplitude of the output voltage is independent of the nature of the load. But the output current waveform as well as magnitude depends upon nature of load impedance. Three phase VSIs are more common for providing adjustable frequency power to industrial applications as compared to single phase inverters. The VSIs take dc supply from a battery or more usually from a 3-phase bridge rectifier.

A basic three phase VSI is a six step bridge inverter, consisting of minimum six power electronics switches (i.e. IGBTs, Thyristors) and six feedback diodes. A step can be defined as the change in firing from one switch to the next switch in proper sequence. For a six step inverter each step is of 60º interval for one cycle of 360º. That means the switches would be gated at regular intervals of 60º in proper sequence to get a three phase ac output voltage at the output terminal of VSI. Fig.2.5 shows the power circuit diagram of three phase VSI using six IGBTs and six diodes connected anti parallel to the IGBTs. The capacitor connected in to the input terminals is to maintain the input dc voltage constant and this also suppresses the harmonics fed back to the dc source. Three phase load is star connected.

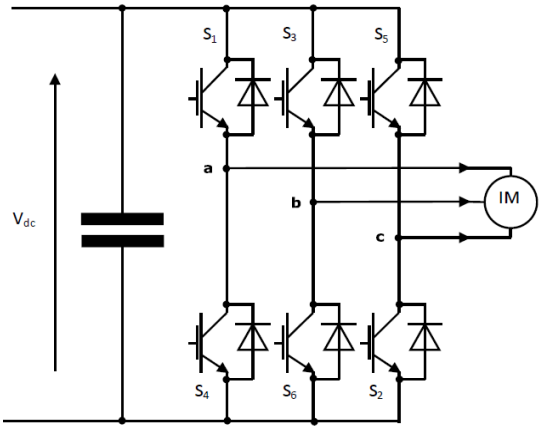

Fig.8 Three phase VSI using IGBTs

The six switches are divided into two groups; upper three switches as positive group (i.e. S1, S3, S5) and lower three as negative group of switches (i.e. S4, S6, S2). There are two possible gating patterns to the switches i.e. there are two conduction modes: 1. 180º conduction mode and 2. 120º conduction mode. In each pattern the gating signals are applied and removed at an interval of 60º of the output voltage waveform. In 180º mode three switches are on at a time, two from positive group and one from negative group or vice versa, each switch conducts for 180º of a cycle. In 120º mode each switch conduct for 120º in one cycle and two switches remain turned on at a time, one from positive group and one from negative group. But no two switches of the same leg should be turned on simultaneously in both cases as this condition would short circuit the dc source.

In 120º conduction mode the chances of short circuit of the dc link voltage source is avoided as each switch conduct for 120º in one cycle, so there is an interval of 60º in each cycle when no switch is in conduction mode and the output voltage at this time interval is zero. In general there is a 60º interval between turning off one switch and turning on of the complimentary switch in the same leg. This 60º interval is sufficient for the outgoing switch to regain its forward blocking capability.

The standard three-phase VSI topology has eight valid switching states which are given in Table.1. Of the eight valid switching states, two are zero voltage states(0 and 7 in Table3.1) which produce zero ac line voltages and in this case, the ac line currents freewheel through either the upper or lower components. The remaining states (1 to 6 in Table3.1) are active states which produce non-zero ac output voltages. The inverter moves from one state to another in order to generate a given voltage waveform. Thus the resulting ac output line voltages consist of discrete values of voltages such $\frac{v_s}{2}$,0 , $-\frac{v_s}{2}$ for the topology shown in Fig. 2.5. The corresponding output voltage waveform is shown in fig.2.6. In 180º mode of conduction the waveform of ac phase output voltage is stepped one having values $\frac{3v_s}{2}$, $\frac{v_s}{2}$. 0, $-\frac{v_s}{2}$. $-\frac{3v_s}{2}$ and line voltage waveform is quasi-square wave type having discrete values$\frac{v_s}{2}$,0 , $-\frac{v_s}{2}$. In 120º mode the phase voltage waveform is quasi-square type.

3. Simulation Results

The output voltage and current waveforms is shown below. This wave form is not constant because of changing temperature. the voltage of each cell is nearly 400 V and current is 1A.

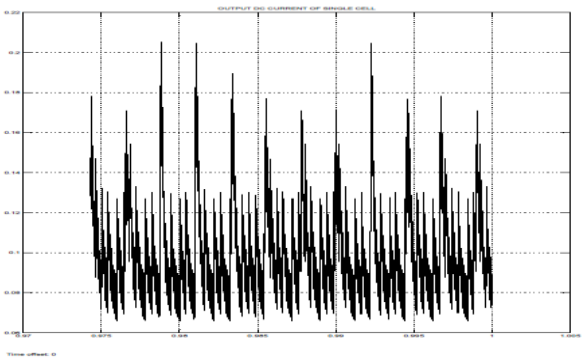

Fig.9 Output Current for Single Cell

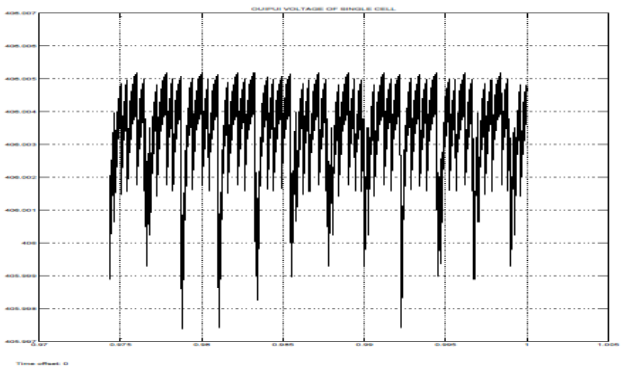

Fig.10 Output Power For Single Cell

Such type of two cells is connected in series for our purpose to produce high voltage. After connecting two cells the output voltage is constant. The wave form of power and voltage generated by the pv system is shown below.

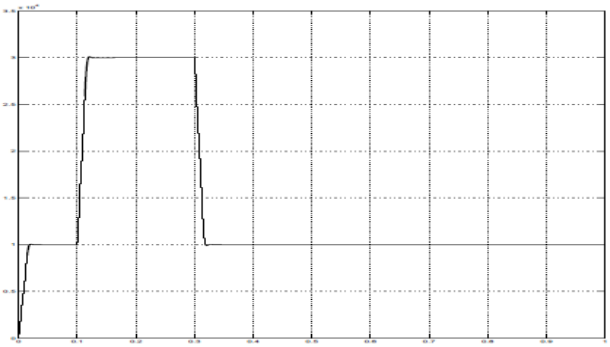

Fig.11 Output power of series connected pv system

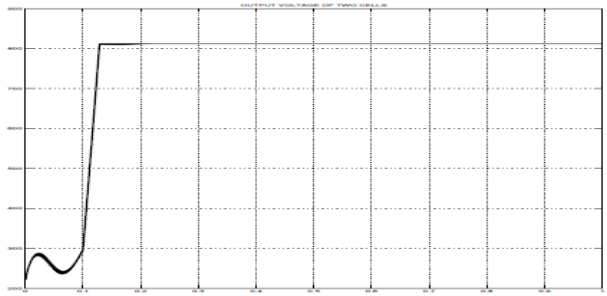

Fig.12 Output voltage of series connected pv system

In this dissertation MPPT technique is used to trap maximum solar power which increases the solar efficiency. By using the MPPT we obtain the constant power which is supply to inverter to drive induction motor. If the solar power generated by the photo voltaic system is not constant then speed does not remains constant. The power generated by solar system is approximately 35000 watt. Which is shown in waveform and voltage is equal to 800 V.

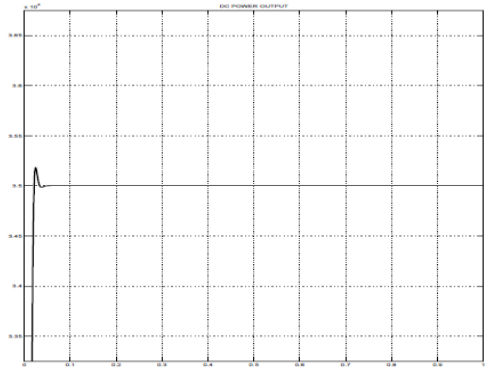

Fig.13 Output power using MPPT

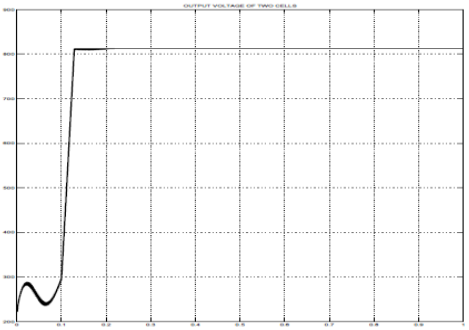

Fig.14 Output voltage using MPPT

After applying the DC voltage to inverter, the inverter convert this into AC voltage. The waveform in shown below

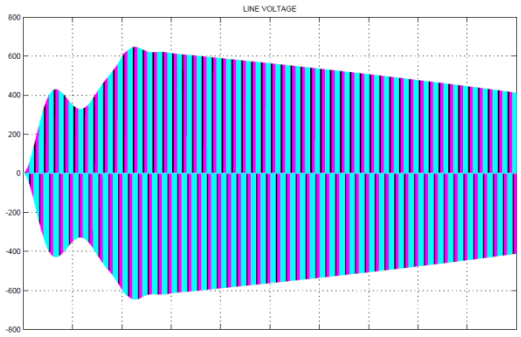

Fig.15 Inverter line Voltage

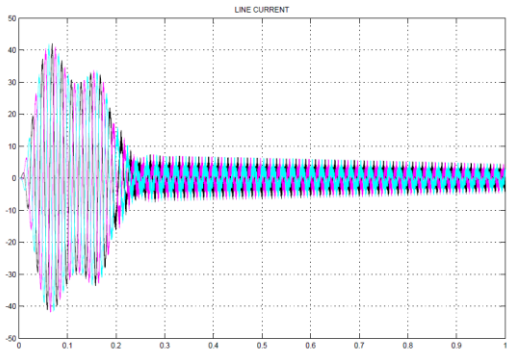

Fig.16 Inverter Line Current

This waveform represents the induction motor rotor and stator current. This voltage and current depends upon the speed of induction motor

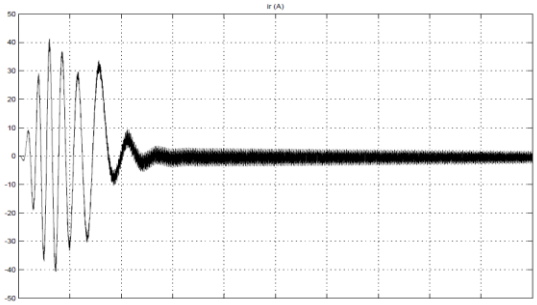

Fig.17 Rotor current

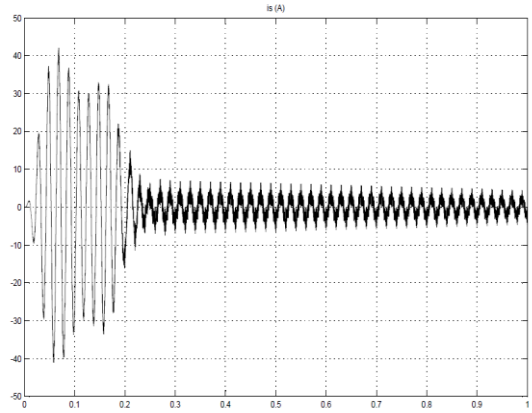

Fig.18 Stator current

Finally, we get the speed of induction motor which is nearly 1500 RPM, this is used to drive any type of electric vehicle. The speed of induction motor can be easily controlled by using semiconductor devices. Now a day induction motor is more popular used in train, car, electric bus etc.

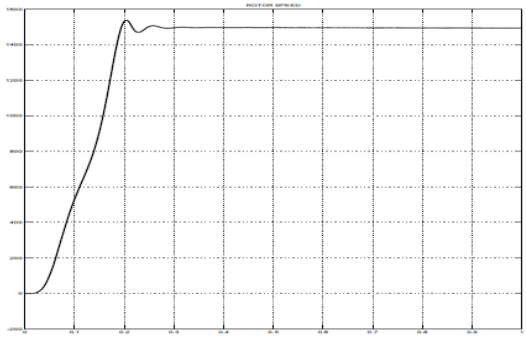

Fig.19 Rotor speed

References

Barrade, P., Delalay (April 2012) S. & Rufer A. Direct connection of super capacitors to photovoltaic panels with on-off maximum power point tracking, *IEEE Trans. Sustainable Energy, vol. 3, no. 2, pp. 283.*

Benavidas N. & Chapman, P. (Nov 2005), Power budgeting of a multiple-input buck boost converter, IEEE Trans. Power Electron., vol. 20, no. 6, pp. 1303– 1309.

Bhattacharya, N. K., Chaudhari S. R. B. & Mukherjee, D. (Jun 2009), PV Embedded grid connected substation for enhancement of energy security, in Proc*. IEEE Photovoltaic Spec. Conf. , pp. 002370–002374.*

Boldue, P., Lehmicke, D. & Smith, J. , (Nov 1993), Performance of a grid connected PV system with Energy storage, *in Proc. IEEE Photovoltaic Spec. Conf., pp. 1159–1162*.

Bragard, M., Soltau, N., Doncker, R. W. D. & Schiemgel, A. (April 2010), Design and implementation of a 5 kW photovoltaic system with Li-ion battery and additional dc/dc converter*, in Proc. IEEE Energy Convers. Congr. , pp. 2944–2949.*

Byrne, J., Wang, Y., Letendre, S. & Govindarajalu, C. (Jun 1994), Deployment of a dispatchable PV system: Technical and economic results, *in Proc. IEEE Photovolt. Spec. Conf., pp. 1200–1203.*

Carbone, R. (Jun 2009), Grid connected PV systems with energy storage, *in Proc. Int. Conf. Clean Electr. Power, pp. 760–767.*

Chiang, S. J., Chang, K. T. & Yen, C. Y. (Jun 1998),Residen tial photovoltaic energy storage system, *IEEE Trans. Ind. Electron., vol. 45, no. 3, pp. 385–394.*

Ding, F., Li, P., Huang, B., Gao, F., Ding, C. & Wang, C. (Jan 2010),Modeling and Simulation of grid connected hybrid PV/battery distributed generation system*, in Proc. China Int. Conf. Electr. Distrib., pp. 1–10.*

Doncker, R. W. D., Meyer, C., Lenke, R. U. & Mura, F. (Nov. 2007),Power Electronics for future utility applications, *in Proc. IEEE 7th Int. Conf. Power Electron. Drive Syst., pp. K-1–K-8.*

Enslin, J. H. & Snyman, D. B. (Jan. 1991 **),**Combined low-cost, high efficient inverter,peak power tracker and regulator for PV applications, *EEETrans. Power Electron., vol. 6, no. 1, pp. 73–82.*

Ertl, H. J., Kolar, W. & Zach, F. (Oct. 2002) ,A novel multi cell dc-ac converter for applications in renewable energy systems, *IEEE Trans. Ind. Electron., vol. 49, no. 5, pp. 1048–1057.*

Ho, C., Breuninger, H., Pettersson, S., Escobar, G., Serpa, L. & Coccia, A. (Jun. 2012),Practical design and implementation procedure of an interleaved boost converter using SiC diodes for PV applications*, IEEE Trans. Power Electron., vol. 27, no. 6, pp. 2835–2845.*

Hu, Y., Tatler, J. & Chen, Z. A (Aug.2004) ,bidirectional DC/DC power electronic converter for an energy storage device in an autonomous power system, *in Proc. IEEE Power Electron. Motion Control Conf., , pp. 171– 176.*

Auzani Jidin, NikIdris, Mohamed Yatim, (Sept Oct 2011),Simple Dynamic Over modulation Strategy For Fast Torque Control in DTC of Induction Machines With Constant-Switching-Frequency Controller, IEEE transactions on industry applications, Vol. 47, No. 5.

Anthony Purcell, P. Acarnley, (may 2001), Enhanced Inverter Switching for Fast Response Direct Torque Control, *IEEE Transactions on Power Electronics, Vol. 16, No. 3.*

A. Mishra, P.Choudhary, (December 2012), Speed Control Of An Induction Motor By Using Indirect Vector Control Method, *IJETAE,Volume 2, Issue 12.*

B. K.Bose. 1997. Power Electronics and Variable Frequency Drives. IEEE Press, New York. Cristian Lascu, Boldea, Blaabjerg (Jan/Feb 2000), A Modified Direct Torque Control for Induction Motor Sensorless Drive*, IEEE transaction on Industry Applications, Vol.36, No.1.*

E.Bassi, P. Benzi, **S.** Buja, (, Sept. Oct. 1992),A Field Orientation Scheme for Current-Fed Induction Motor Drives Based on the Torque Angle Closed-Loop Control, *IEEE Transactions on Industry Applications*, Vol. 28, No. 5